



S2 Genomics
From Samples to Genomics

APPLICATION NOTE

Single-Cell Sequencing of Tumor-Infiltrating Lymphocytes in Lung Cancer: A Comparative Analysis Using the Singulator™ Platform

Abstract

In the realm of cancer immunotherapy, understanding the complex interactions between tumors and the immune system is crucial for devising effective treatment strategies. Tumor-infiltrating lymphocytes (TILs) play a pivotal role in the anti-tumor immune response and can serve as valuable indicators of patient prognosis and therapeutic response. The advent of advanced single-cell sequencing technologies has revolutionized the field by enabling comprehensive profiling of TIL populations. Here, we demonstrate the use of the Singulator™ Platform to generate high quality single-cell suspensions from normal and tumor human lung tissue with up to 94% viability. These suspensions were used as input to the 10x Single Cell 3' v3.1 Gene Expression Assay and to purify TILs from the tumor samples using immunogenic bead separation, demonstrating the epitopes remain intact on the surface of the TILs through the Singulator™ process. Finally, we characterized the gene expression differences between matched normal lung tissues, tumor samples and TILs from 3 patients and identified a gene expression profile that is specific to the TILs purified from the tumor samples.

Introduction

Cancer immunotherapy using TILs is a new and exciting field that leverages the body's own immune system to fight cancer, offering new hope to patients with various types of cancers. TILs are a type of immune cell, including T-cells, B-cells, and Natural Killer cells (NK cells), that have recognized the tumor as foreign and have infiltrated the tumor to attack the cancer cell. TILs play a significant role in the anti-tumor immune response and can be valuable indicators of patient prognosis and therapeutic response.

In this Application Note, we demonstrate how the Singulator™ platform can be used to generate single-cell suspensions that are suitable for downstream applications like immunomagnetic positive selection methods based on cell surface epitopes and single-cell gene expression assays. We isolated cells from squamous cell carcinoma and adenocarcinoma tumors and adjacent normal lung tissue using the Singulator™ Platform. TILs from the dissociated tumor cells were then isolated using an immunomagnetic positive selection kit from Stemcell™ technologies that recognizes CD45+ cells. scRNA-seq using 10x Genomics™ 3' GEX technology was performed on all three samples – normal lung, tumor and TILs – to investigate the cellular transcriptome. Cell types were characterized, and differential gene expression was analyzed using Seurat v5 to investigate the gene expression differences between normal T-cells vs. TILs isolated from the tumor microenvironment.

First, we confirmed the Singulator™ Platform's performance, including the reproducibility and precision of the Singulator™ Platform to generate single-cell suspensions from biological replicates. This allowed us to estimate cellular composition differences in healthy vs cancerous tissues and simultaneously measure the gene expression profiles.

Next, we analyzed differential gene expression between normal natural killer lymphocyte cells (NK cells) and those from the tumor microenvironment, finding genes of interest for further investigation impacting the anti-tumor response. By combining the power of high-throughput single-cell analysis with streamlined sample preparation, this approach promises to enhance our understanding of tumor immunology, aiding in the development of personalized cancer therapies.

Methods

Experimental Design

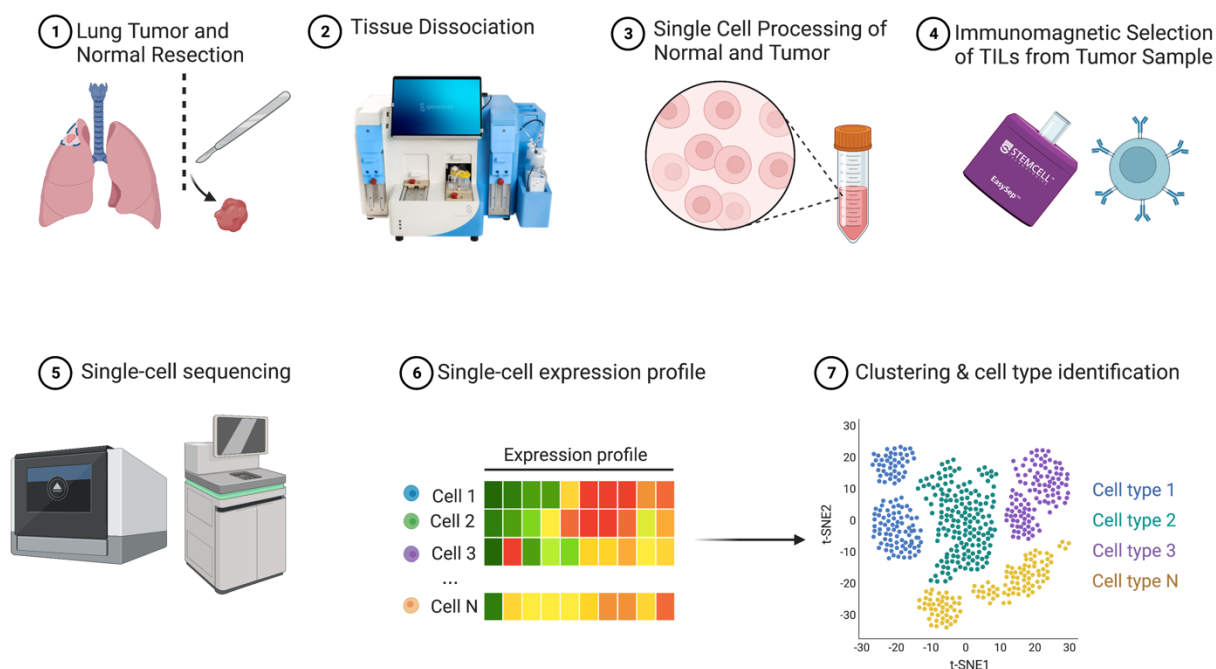


Figure 1. Experimental Design. Normal lung and tumor tissues were dissociated into a single-cell suspension with a Singulator™ 100. The yields and viabilities of the cells were measured. Tumor cells were then used to isolate tumor infiltrating leukocytes (TILs) via EasySep™ Release Human CD45+ Selection Kit (Stemcell™ Technologies). 10,000 cells were targeted with the 10x Genomics™ Next GEM Single Cell 3' Kit v3.1. Sequencing data were analyzed with 10x Genomics' Cell Ranger v7 and Seurat v5.

Sample Preparation

Fresh human lung normal and squamous cell carcinoma tumor tissue (260 mg and 250 mg) from 2 patients, and fresh human lung normal and adenocarcinoma (130 mg) from a third patient were procured from the Cooperative Human Tissue Network (CHTN) and received cold in RPMI buffer through overnight shipment. Accurate mass measurements for normal lung tissue were not determined due to swelling and enlargement from buffer uptake during shipment. The normal lung and tumor samples were finely minced and processed in the Singulator™ 100 (S100) using the Lung Cell Isolation protocol, Lung Isolation Reagent (100-064-413), Tumor Isolation Reagent (100-247-099), and Cell Isolation Cartridges (100-063-178). The detailed protocol is described in the Cell Isolation Protocol Guide (100-249-015) starting on page 49.

The resulting single-cell suspensions were removed from the cartridge and centrifuged at 300 g for 5 minutes at 4 °C. Red blood cells (RBCs) were lysed with ACK RBC Lysis Buffer for 5 minutes at 4 °C. Small debris was removed by density gradient centrifugation. Cell pellets were resuspended in DMEM.

Yield counts and viability were determined via AO/PI staining using the Nexcelom K2. A 100 mL solution at 1,200 cells per mL was made for each sample in DMEM + 10% FBS. The remaining tumor cells were taken through TILs isolation using the EasySep™ Release Human CD45 Positive Selection Kit (StemCell™ Technologies Catalog # 100-0105) following the manufacturer's recommended instructions. The isolated TILs were counted, and viability were determined via AO/PI staining using the Nexcelom K2. A 100 mL solution at 1,200 cells per mL was made in DMEM + 10% FBS. The normal lung, tumor, and TILs cells were processed using the 10x Genomics™ Next GEM Single Cell 3' Kit v3.1 targeting 10,000 cells.

Sequencing

All cell preps were processed using the 10x Genomics™ Next GEM Single Cell 3' Kit v3.1 targeting 10,000 cells. Libraries were sequenced on an Illumina NovaSeq 6000.

Data Analysis

Data was processed with Cell Ranger v7 using default settings to generate raw and filtered feature matrices.

Before quality control, the raw data were preprocessed using SoupX¹⁷ to remove ambient RNA contamination and DoubletFinder⁹ to identify and exclude potential doublet cells. These steps ensure subsequent analyses are performed on clean data, representing individual, uncontaminated cells.

After preprocessing, the data was subjected to quality control using Seurat v5.0⁶. Cells were filtered out if they had mitochondrial gene expression over 10% for normal lung and TILs cells, and over 15% for tumor cells. Additionally, cells were removed if they had fewer than 500 or more than 6,000 unique feature counts. Following QC, the data was then normalized using SCTransform v2 to prepare for integration. Following normalization, the 3 normal lung, tumor and TILs cells were then integrated with each other via Harmony⁶. Dimensionality reduction was then performed using principal component analysis (PCA) considering the top 30 principal components, UMAPs were generated, and cells were clustered to Seurat resolution of 0.3. normal lung, tumor, and TILs manually annotated using marker genes from published literature^{1-4, 11-16}.

Results

Singulator Derived Cell Preps

Normal lung cell isolation yielded 674,000, 2,635,000 and 645,000 cells at 94%, 96%, and 82% for patients 1,2 and 3, respectively. Tumor cell isolation yielded approximately 6,731,920, 5,065,000, and 2,787,460 cells at 94%, 99%, and 90% viability for patients 1,2 and 3, respectively. TILs post-isolation using the Stemcell™ EasySep™ Kit yielded between 145,000 – 1,312,000 cells from an input of all remaining tumor cells after 10x Chip loading from the tumor cell suspension. Viability (**Figure 2 A, C**) and yield (**Figure 2 B, D**) of normal lung samples and cancer samples were determined, respectively. Representative images of single-cell suspensions from patients 1, 2 and 3 (**Figure 3**).

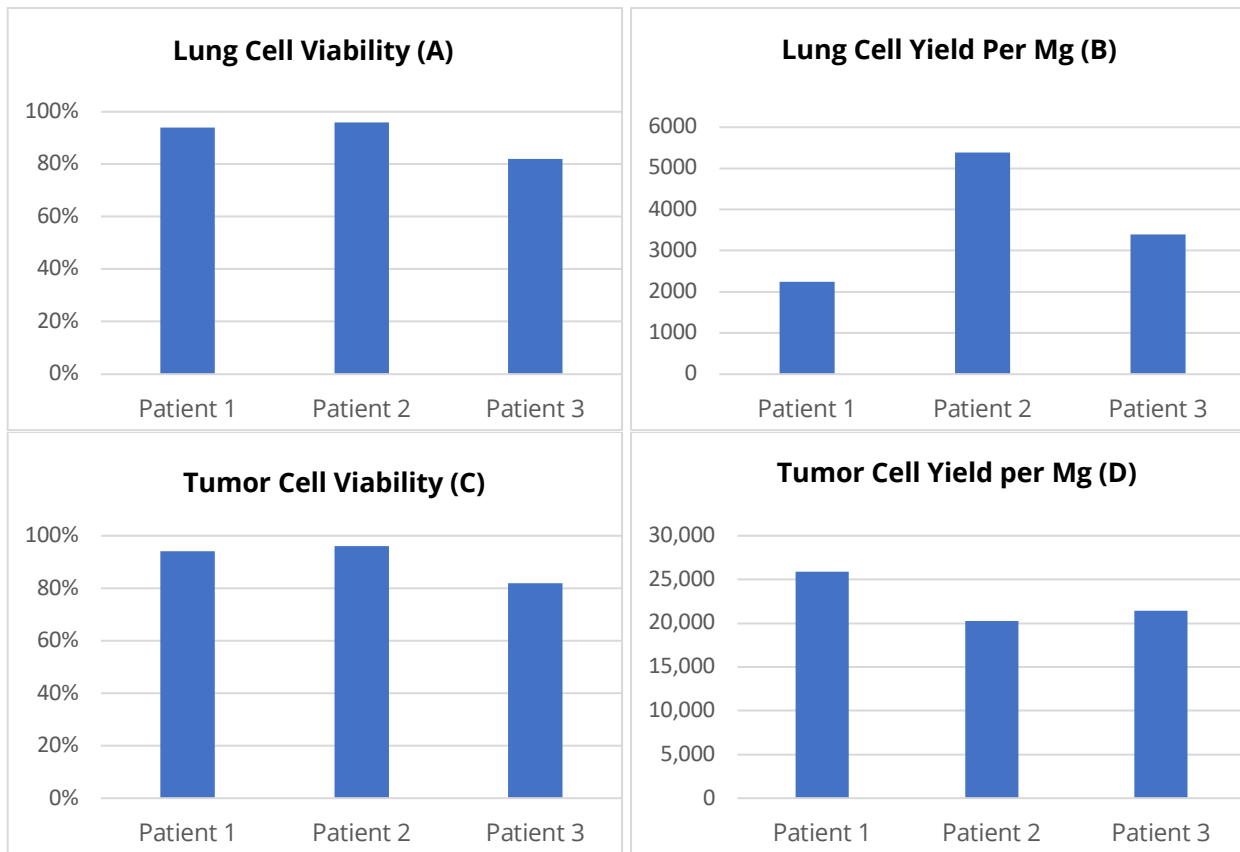


Figure 2: Viability and yield for normal lung samples and tumor samples.

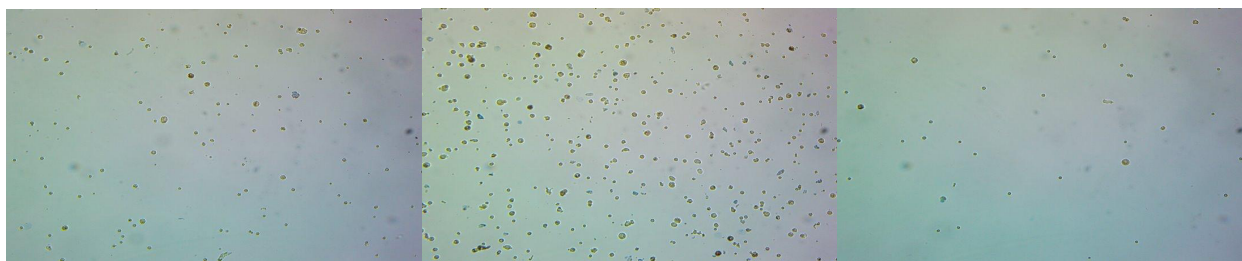


Figure 3. Cell Prep Images. 10x magnified images of patient 1 cell preps stained with Trypan Blue. (Left to right: normal lung cells, tumor cells, and TILs)

Cell Analysis

Detailed number of cells and median transcripts, genes and reads per cell information are in Table 1 for each patient. Normal lung, tumor, and TILs samples were then integrated and UMAPs were generated as described in methods with broad cell type labeling according to published marker genes^{1-4, 11-16}. For the normal lung cell sample, 12 cell types were identified and labeled including a variety of endothelial and immune cells. In the tumor cell sample, 6 general cell types were identified and labeled including a cancer cell cluster identified via cancerous marker genes EPCAM, EGFR, and KRAS^{4,15}. 5 major cell types were identified in the TILs sample including the major T-cell populations, B-cell, monocyte, macrophage and pericyte populations (**Figure 4**). Next, for normal lung cells we determined the fraction of cells from each cell type in each library for (**Figure 5**) to examine the reproducibility of the isolations.

Patient	Sample	# of cells recovered	Median Transcripts per cell	Median Genes per cell	Reads per cell
1	Normal Lung	6831	2,961	1,408	15,811
	Tumor	8500	4,355	1,459	28,345
	TILs	8,668	3,614	1,302	22,748
2	Normal Lung	6716	4,937	1,949	31,019
	Tumor	6,458	5,441	1,936	26,835
	TILs	6,192	3,682	1,302	25,962
3	Normal Lung	5,960	5,036	2,198	33,388
	Tumor	8,191	4,213	1,723	27,394
	TILs	8,054	4,080	1,650	20,205

Table 1: Sequencing metrics for each sample type by patient. Including number of cells sequenced, median transcripts, median genes, and median reads per cell.

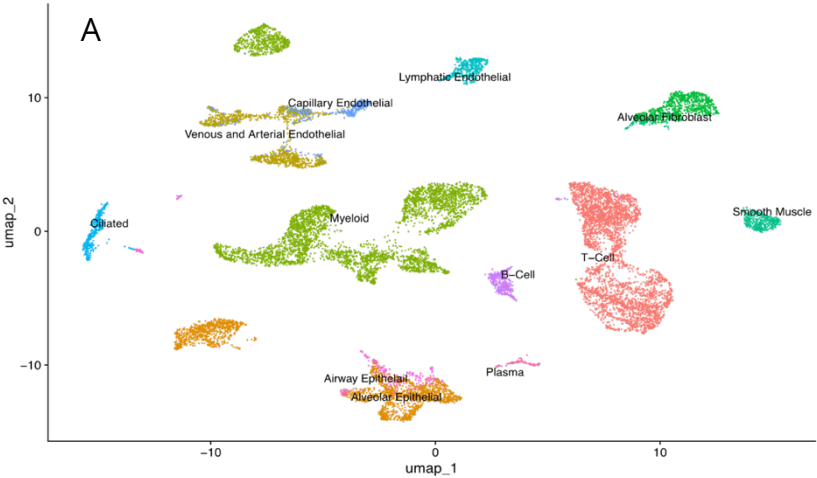
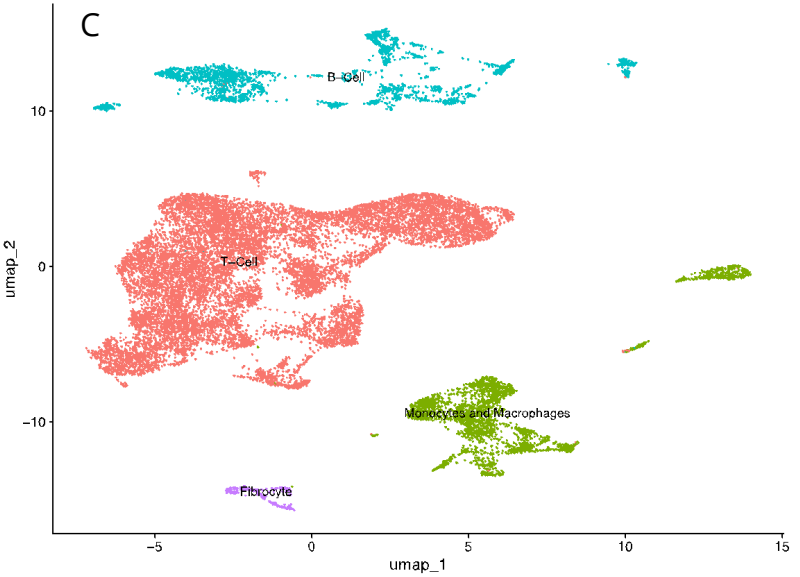
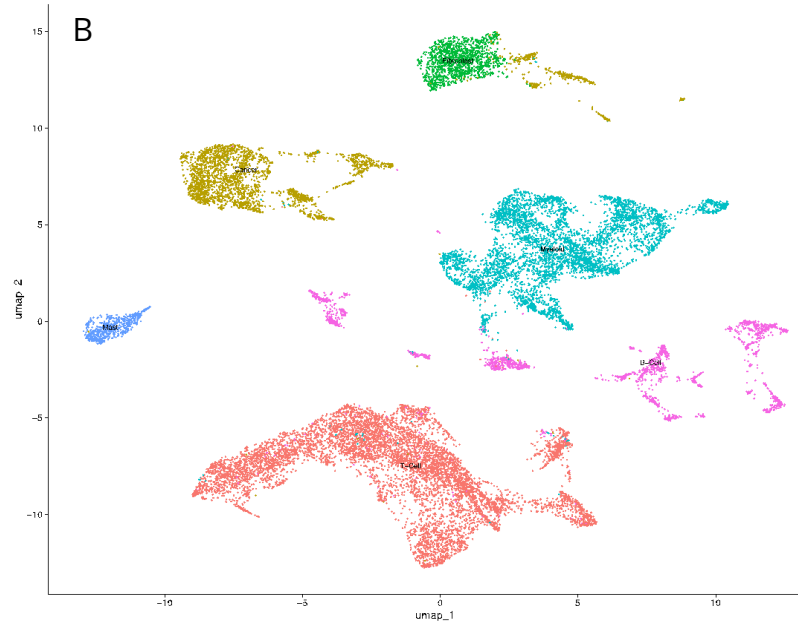


Figure 4: UMAP clustering of normal lung (A), tumor (B), and TILs (C). Cells from each patient were QC'd, integrated, visualized as UMAPs, and clustered. Cell types were identified by canonical marker gene expression.



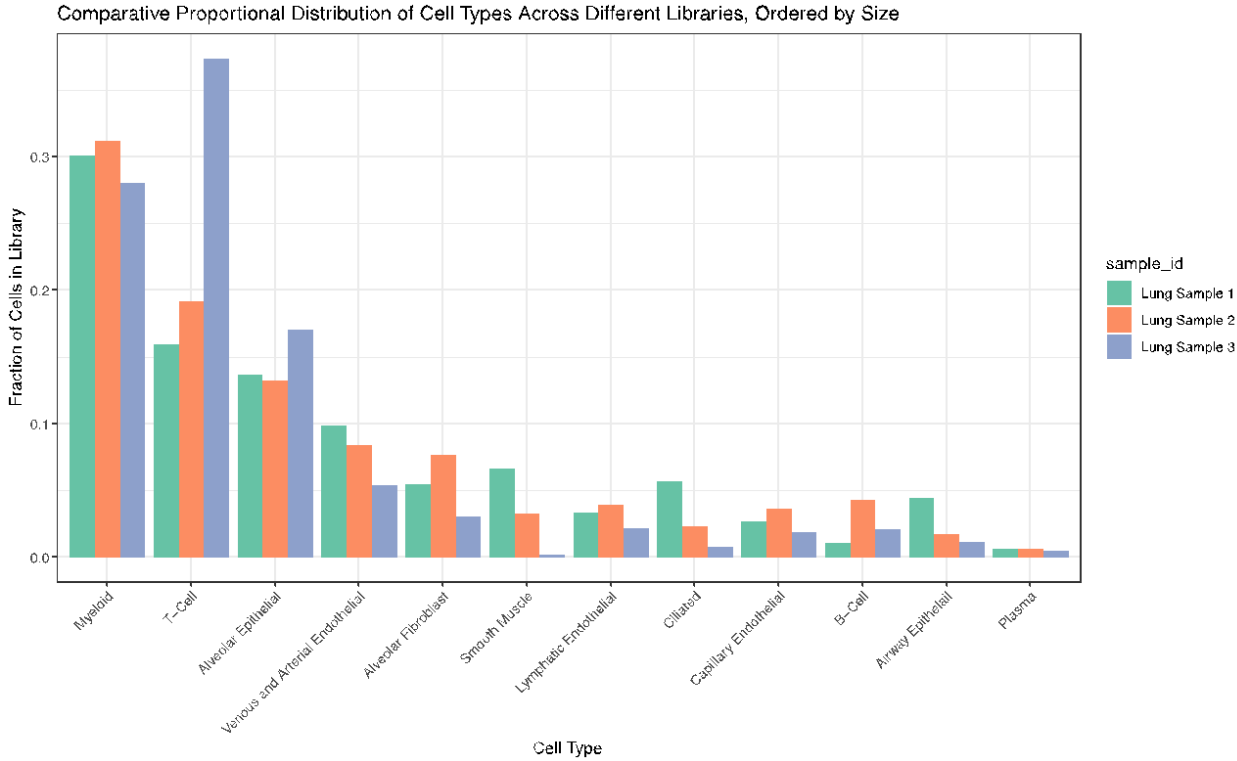


Figure 5: Fraction of Cells in Normal Lung Samples. Distribution of cell types across each patient’s normal lung cells. Showing reproducible proportions of myeloid, immune, epithelial, endothelial, and other types isolated across biological replicates.

Reproducibility of Singulator Prepared Normal Lung Cell Preps

Normal lung samples were down-sampled to 15,800 reads per cell and QC information including genes per cell, transcripts per cell and mitochondrial contamination for each patient was determined (**Figure 6**). Finally, we generated Pearson correlation coefficients from pseudo-bulk average gene expression across the individual samples. All 3 human lung normal libraries showed similar QC information, cell type representation proportions (**Figure 6**), and Pearson correlations equal to or above 0.936 for average gene expression (**Figure 7**).

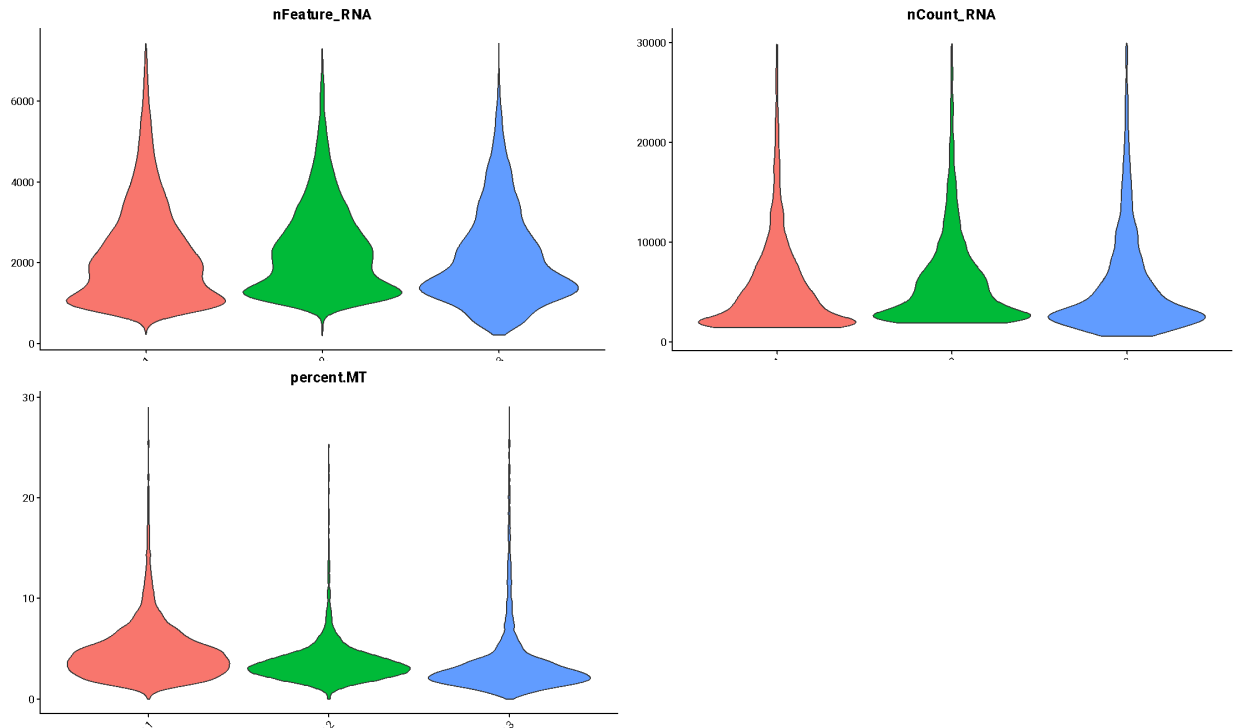


Figure 6: QC metrics including genes per cell (nFeature_RNA), UMI per cell (nCount_RNA), and mitochondrial contamination (percent.MT) for down-sampled normal lung samples for patients 1,2 and 3.

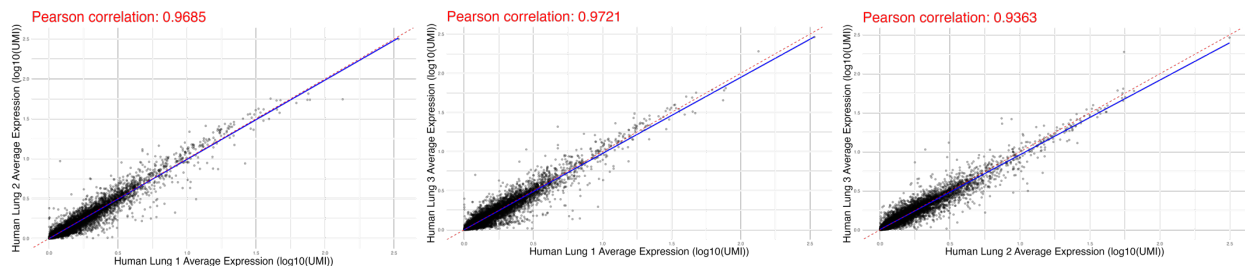


Figure 7: Average expression graphs with Pearson correlations showing reproducibility of the cell preps across patients' down-sampled normal lung cells.

Preservation of the CD-45 Epitope for positive selection

CD45 is a transmembrane protein found on the surface of all nucleated hematopoietic cells and can be used to isolate TIL from solid tumors⁵. The EasySep™ Release CD45 Positive Selection Kit from Stemcell™ Technologies binds specifically to leukocytes, allowing for their selective identification and separation from other cell types in the tumor microenvironment. The combination of rapid tumor dissociation via the Singulator™ and surface epitope preservation allows for TILs isolation and expands access for TILs research.

When integrating the three patient tumor samples with the TILs datasets and comparing the gene expression feature plot of PTPRC, the gene responsible for encoding the CD-45 receptor, we can see the successful isolation of CD-45 positive cells away from other tumor cells (**Figure 8A**). We then integrated all three TILs datasets and used published marker genes^{1,13,14} for T-cells, B-cells, monocytes, macrophages, and fibrocytes to confirm isolation of CD-45 positive cell types (**Figure 8B**).

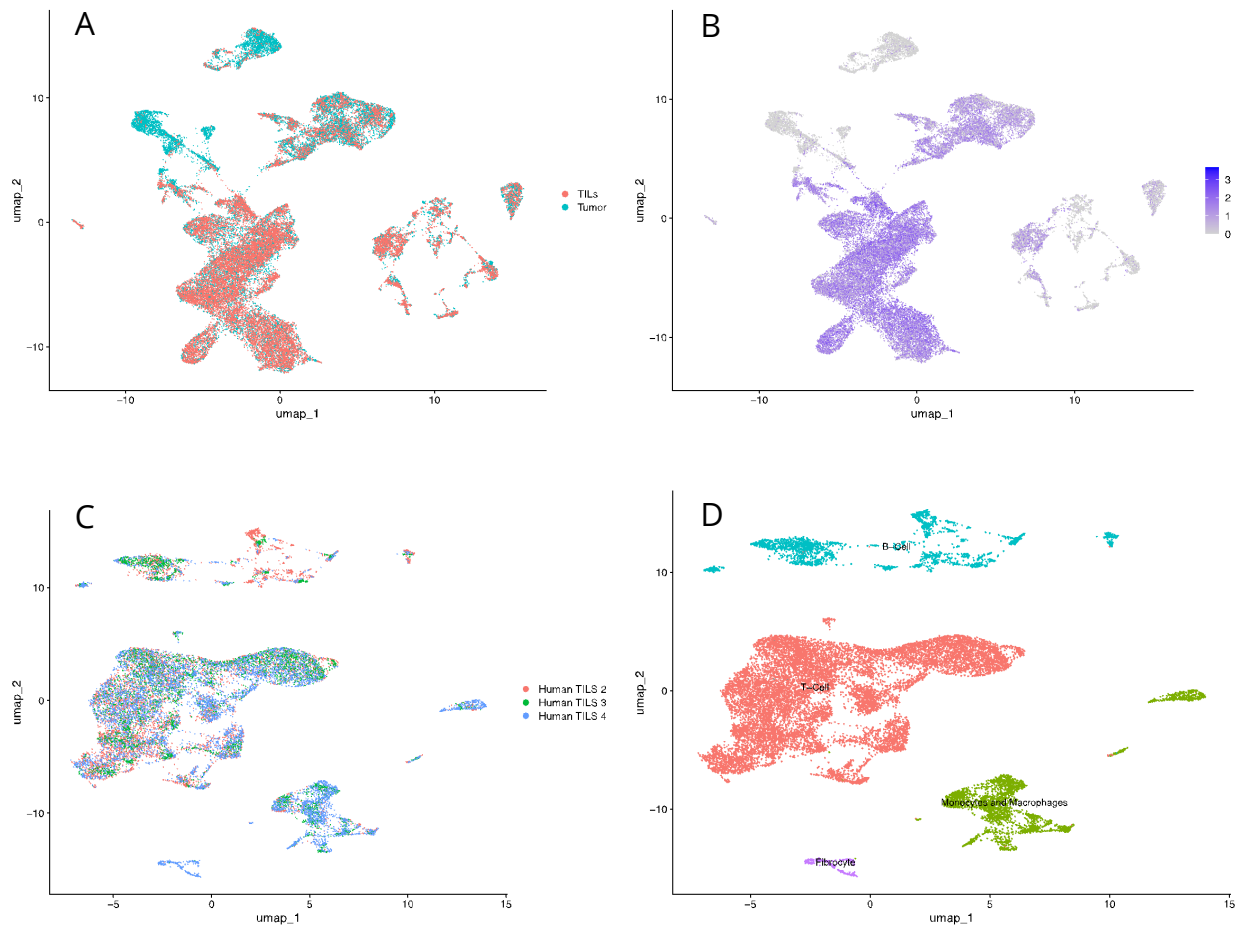


Figure 8. (A) Integrated UMAP of all three patient TILs and tumor samples with PTPRC gene feature plot showing positive isolation of CD-45 cells from tumor samples. (B) Integrated TILs sampling and cell type labeling showing 5 major cell types associated with CD-45 receptor expression.

Differential Gene Expression between T-cells in Normal and Cancer Samples

Finally, we identified genes that are differentially expressed between T-cells found in normal lung and tumor samples. First, normal lung and TILs samples from all three patients were integrated, clustered, and reanalyzed. (**Figure 9A**). A subset of T-cells was then identified by marker gene CD3D (**Figure 9B**), reclustered and visualized by the original population: normal lung or TILs (**Figures 9C & 9D**). The T-cells cluster was chosen based on their contribution to the antitumor response¹⁴.

Differential gene expression analysis was completed, finding the top 10 most differentially expressed genes between the normal lung and TILs datasets for the T-cells' cluster visualized as a volcano plot (**Figure 9E**). The top 10 differentially expressed genes identified were RPS20, FGF2P2, TYROBP, AOA, SPON2, FCGR3A, HSP90AB1, KLR1, RPL13A, SFTPC.

Of the top 10 genes identified, we further investigated FCGR3A AND HSP90AB1. HSP90 inhibitor has previously been described to inhibited tumor cell growth and induced apoptosis without obvious side effects in lung tumor xenograft models.¹⁰

FCGR3A gene has been confirmed to be involved in immune cell infiltration, immune checkpoint genes, and DNA mismatch repair genes expression in carcinoma samples⁸. These genes warrant further investigation by researchers for their role as potential molecular targets for T-cells in the tumor microenvironment.

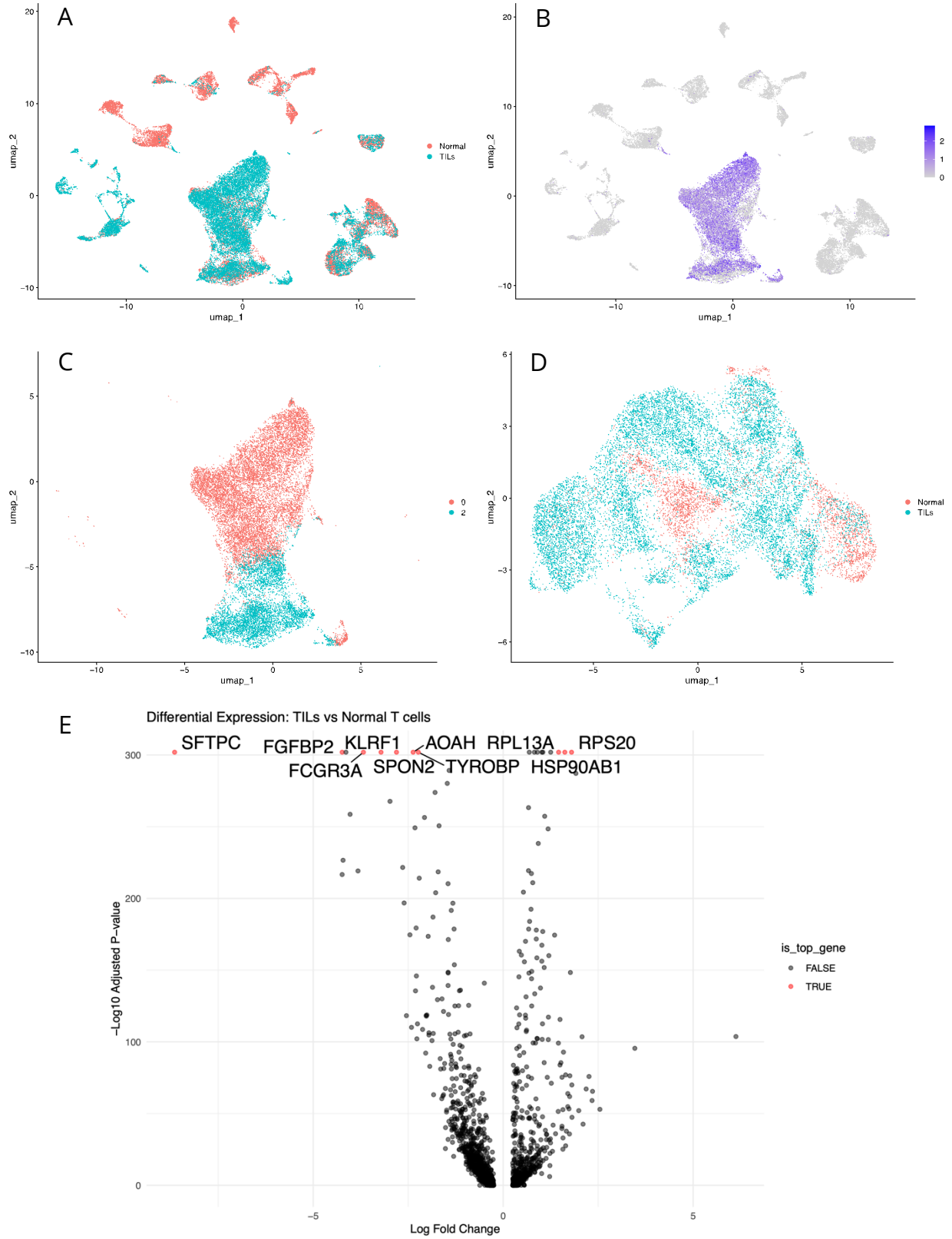


Figure 9: (A) Integration and UMAP of TILs and normal lung datasets for all three patients, (B) CD3D T-cell marker gene expression (C) T-cell subset clusters, (D) T-Cell subset reclustered and separated by normal and TILs sample sets (E) Volcano plot showing differentially expressed genes of T-cells normal vs. TILs populations with top 10 genes labeled.

Conclusion

These data demonstrate the ability of the Singulator Platform to prepare single-cell suspensions for both positive selection by a cell surface marker and single-cell RNA sequencing. These methods enable researchers to identify genes of interest for potential therapeutic targets for anti-tumor response.

Expanding access to the sequencing of TILs provides valuable information about the diversity and functional states of individual immune cells within the tumor. This plays a crucial role in advancing our understanding of cancer biology and the development of personalized cancer therapies. The ability to process both normal lung and tumor samples with preconfigured kits and protocols allows for increased throughput and ease in investigating the relationship between the normal and tumor microenvironments. Comparison of gene expression between TILs and normal leukocytes can provide insights into the complex interplay between the immune system and cancer, identifying potential biomarkers, therapeutic targets, and predictive indicators for patient outcomes.

References

1. Bischoff, P., Trinks, A., Obermayer, B. *et al.* Single-cell RNA sequencing reveals distinct tumor microenvironmental patterns in lung adenocarcinoma. *Oncogene* **40**, 6748–6758 (2021). doi: <https://doi.org/10.1038/s41388-021-02054-3>
2. Deprez M, Zaragosi LE, Truchi M, et al. A Single-Cell Atlas of the Human Healthy Airways. *Am J Respir Crit Care Med.* 2020;202(12):1636-1645. doi: <https://doi.org/10.1164/rccm.201911-2199OC>
3. DeNardo DG, Andreu P, Coussens LM. Interactions between lymphocytes and myeloid cells regulate pro- versus anti-tumor immunity. *Cancer Metastasis Rev.* 2010;29(2):309-316. doi: <https://doi.org/10.1007/s10555-010-9223-6>
4. Dogan S, Shen R, Ang DC, et al. Molecular epidemiology of EGFR and KRAS mutations in 3,026 lung adenocarcinomas: higher susceptibility of women to smoking-related KRAS-mutant cancers. *Clin Cancer Res.* 2012;18(22):6169-6177. doi: <https://doi.org/10.1158/1078-0432.CCR-11-3265>
5. Harfmann, M., Schröder, T., Głów, D., Jung, M., Uhde, A., Kröger, N., Horn, S., Riecken, K., Fehse, B., & Ayuk, F. A. (2024). CD45-Directed CAR-T Cells with CD45 Knockout Efficiently Kill Myeloid Leukemia and Lymphoma Cells In Vitro Even after Extended Culture. *Cancers*, *16*(2), 334. doi: <https://doi.org/10.3390/cancers16020334>
6. Hao, Y., Stuart, T., Kowalski, M.H. *et al.* Dictionary learning for integrative, multimodal and scalable single-cell analysis. *Nat Biotechnol* **42**, 293–304 (2024). <https://doi.org/10.1038/s41587-023-01767-y>
7. Korsunsky, I., Millard, N., Fan, J. *et al.* Fast, sensitive and accurate integration of single-cell data with Harmony. *Nat Methods* **16**, 1289–1296 (2019). doi: <https://doi.org/10.1038/s41592-019-0619-0>
8. Li, L., Huang, Z., Du, K., Liu, X., Li, C., Wang, D., Zhang, Y., Wang, C., & Li, J. (2022). Integrative Pan-Cancer Analysis Confirmed that FCGR3A is a Candidate Biomarker Associated With Tumor Immunity. *Frontiers in pharmacology*, *13*, 900699. doi: <https://doi.org/10.3389/fphar.2022.900699>
9. McGinnis CS, Murrow LM, Gartner ZJ. DoubletFinder: Doublet Detection in Single-Cell RNA Sequencing Data Using Artificial Nearest Neighbors. *Cell Syst.* 2019 Apr 24;8(4):329-337.e4. doi: <https://doi.org/10.1016/j.cels.2019.03.003> . Epub 2019 Apr 3. PMID: 30954475; PMCID: PMC6853612.
10. Niu, M., Zhang, B., Li, L., Su, Z., Pu, W., Zhao, C., Wei, L., Lian, P., Lu, R., Wang, R., Wazir, J., Gao, Q., Song, S., & Wang, H. (2022). Targeting HSP90 Inhibits Proliferation and Induces Apoptosis Through AKT1/ERK Pathway in Lung Cancer. *Frontiers in pharmacology*, *12*, 724192. doi: <https://doi.org/10.3389/fphar.2021.724192>
11. Salcher S, Sturm G, Horvath L, et al. High-resolution single-cell atlas reveals diversity and plasticity of tissue-resident neutrophils in non-small cell lung cancer. *Cancer Cell.* 2022;40(12):1503-1520.e8. doi: <https://doi.org/10.1016/j.ccell.2022.10.008>
12. Schupp JC, Adams TS, Cosme C Jr, et al. Integrated Single-Cell Atlas of Endothelial Cells of the Human Lung. *Circulation.* 2021;144(4):286-302. doi: <https://doi.org/10.1161/CIRCULATIONAHA.120.052318>
13. Stankovic B, Bjørhovde HAK, Skarshaug R, et al. Immune Cell Composition in Human Non-small Cell Lung Cancer. *Front Immunol.* 2019;9:3101. Published 2019 Feb 1. doi: <https://doi.org/10.3389/fimmu.2018.03101>
14. Wang, C., Yu, Q., Song, T. *et al.* The heterogeneous immune landscape between lung adenocarcinoma and squamous carcinoma revealed by single-cell RNA sequencing. *Sig Transduct Target Ther* **7**, 289 (2022). doi: <https://doi.org/10.1038/s41392-022-01130-8>
15. Wu, F., Fan, J., He, Y. *et al.* Single-cell profiling of tumor heterogeneity and the microenvironment in advanced non-small cell lung cancer. *Nat Commun* **12**, 2540 (2021). doi: <https://doi.org/10.1038/s41467-021-22801-0>
16. Xu Y, Mizuno T, Sridharan A, et al. Single-cell RNA sequencing identifies diverse roles of epithelial cells in idiopathic pulmonary fibrosis. *JCI Insight.* 2016;1(20):e90558. Published 2016 Dec 8. doi: <https://doi.org/10.1172/jci.insight.90558>
17. Young MD, Behjati S (2020). "SoupX removes ambient RNA contamination from droplet-based single-cell RNA sequencing data." *GigaScience*. doi: <https://doi.org/10.1093/gigascience/giaa151>